

Development of Selective Inhibitors and Substrate of Matrix Metalloproteinase-12*

Received for publication, January 10, 2006, and in revised form, February 13, 2006. Published, JBC Papers in Press, February 15, 2006, DOI 10.1074/jbc.M600222200

Laurent Devel[‡], Vassilis Rogakos[§], Arnaud David[‡], Anastasios Makaritis[§], Fabrice Beau[‡], Philippe Cuniasse[‡], Athanasios Yiotakis[§], and Vincent Dive^{‡1}

From the [‡]Commissariat à l'Energie Atomique, Département d'Ingénierie et d'Etudes des Protéines Bat 152, CE-Saclay, 91191 Gif/Yvette, Cedex, France and the [§]Laboratory of Organic Chemistry, Department of Organic Chemistry, University of Athens, Panepistimiopolis, Zografou, 15771 Athens, Greece

Four phosphinic peptide libraries with compounds having the general formula $p\text{-Br-Ph}-(\text{PO}_2\text{-CH}_2)\text{-Xaa}'\text{-Yaa}'\text{-Zaa}'\text{-NH}_2$ have been prepared and screened against 10 matrix metalloproteinases (MMPs). We identified two phosphinic peptides with K_i values of 0.19 and 4.4 nM toward MMP-12 (macrophage elastase) that are more than 2–3 orders of magnitude less potent toward the other MMPs tested. These highly selective MMP-12 inhibitors contain a Glu-Glu motif in their Yaa'-Zaa' positions. Incorporation of this Glu-Glu motif into the sequence of a nonspecific fluorogenic peptide cleaved by MMPs provides a highly selective substrate for MMP-12. A model of one of these inhibitors interacting with MMP-12 suggests that the selectivity observed might be due, in part, to the presence of two unique polar residues in MMP-12, Thr²³⁹ and Lys¹⁷⁷. These MMP-12-selective inhibitors may have important therapeutic applications to diseases in which MMP-12 has been suggested to play a key role, such as in emphysema, atherosclerosis, and aortic abdominal aneurysm.

The matrix metalloproteinases (MMPs)² form a group of structurally related extracellular zinc endoproteases able to degrade at least one protein component of the extracellular matrix (1). Based on this property, MMPs are considered to be critical mediators of both normal and pathological tissue remodeling processes (2, 3). Their overexpression is observed in and associated with a variety of diseases, including cancer (4, 5), arthritis (6), multiple sclerosis (7, 8), and atherosclerosis (9, 10). Therefore, there is substantial interest in developing MMP synthetic inhibitors for a variety of therapeutic indications (11–15). Results of the first clinical trials with broad spectrum MMP inhibitors in cancer therapy were disappointing, highlighting the need for better understanding of the exact role of each MMP during the different stages of tumor progression (16). Recent research in this field has focused on the development of inhibitors that fully differentiate one MMP from another (17). This is a particularly difficult task, since the topology and nature of the residues in the enzyme's active site are highly conserved among the different MMPs (18). Moreover, parts of the MMP catalytic domain, which play a critical role in enzyme specificity, seem to be highly flexible

(19, 20). This situation may explain why most previously reported MMP synthetic inhibitors preferentially inhibit some MMPs but are not exclusive inhibitors of a single MMP. A recent breakthrough in this field was achieved by identifying the first highly selective synthetic inhibitor of MMP-13 (21). Selective inhibitors for MMP-2 and MMP-9 have also been reported recently, but their degree of selectivity toward MMPs is less than that achieved for the MMP-13-selective inhibitor (22).

To identify highly selective MMP inhibitors, libraries of phosphinic peptides were prepared. Phosphinic peptides are good transition state mimics and have been shown to behave as highly potent inhibitors of different zinc metalloproteinases (23). To probe the S'_1 cavity of MMPs, a chemical strategy that makes it possible to prepare phosphinic peptides harboring various substituents in their P'_1 position was used (see Scheme 1). This strategy relies on the use of a common precursor, which can be modified in one step, to prepare phosphinic peptides displaying substituted isoxazole side chains in their P'_1 position (24). In such phosphinic peptides, the isoxazole ring is used as a rigid scaffold to project in the right orientation various chemical groups able to interact with the S'_1 subsite of MMPs, which corresponds to a deep cavity. Based on this strategy, four libraries of phosphinic peptides, containing four different isoxazole side chains in their P'_1 position, were prepared by introducing additional chemical diversity in the P'_2 and P'_3 positions of the inhibitors (see Scheme 1). Screening of these libraries against 10 different MMPs allowed us to identify highly selective inhibitors of MMP-12. Based on the unique structure of these inhibitors, a highly selective substrate of MMP-12 has been developed, and determinants of MMP-12 selectivity have been tentatively mapped by developing a model of interaction of one of these selective inhibitors with MMP-12.

EXPERIMENTAL PROCEDURES

Commercial reagents were used as received without additional purification. Solvents were of the reagent grade available from commercial sources and used without further purification. SynPhase lanterns[®], colored cogs, and spindles were from Mimotopes. Fmoc-amino acids were from Novabiochem. N,N' -diisopropylcarbodiimide (DIC), N -hydroxybenzotriazole (HOBt), trifluoroacetic acid, and triisopropylsilane were from Aldrich. N^2 -Fmoc- N^3 -2,4-dinitrophenyl-L-2,3-diaminopropionic acid and (7-methoxycoumarin-4-yl)acetyl (Mca) were from Bachem. Anhydrous N,N -dimethyl formamide (DMF) was from Fluka. Mca-Pro-Leu-Gly-Leu-Dpa-Ala-Arg-NH₂ was from Novabiochem. Catalytic domains of mouse MMP-11, human MMP-7, and MMP-14 expressed in *Escherichia coli* BL21 DE3 pLysS cells were obtained and purified as described before (25). All of the other human MMPs were from R&D Systems. Analytical and preparative reverse phase HPLC separations were respectively performed on a Thermo separation product and Gilson apparatus using AIT C₁₈ Kromasil (250 × 4.6 mm) and AIT C₁₈ Kromasil (250 × 20 mm) columns with a flow rate of 1 and 3

* This work was supported by funds from the Commissariat à l'Energie Atomique and from the European Commission FP5RDT (QLK3-CT02-02136) and FP6RDT (Cancer Degradome project, LSHC-CT-2003-503297). The costs of publication of this article were defrayed in part by the payment of page charges. This article must therefore be hereby marked "advertisement" in accordance with 18 U.S.C. Section 1734 solely to indicate this fact.

¹ To whom correspondence should be addressed. Tel.: 33-1-69083585; Fax: 33-1-69089071; E-mail: vincent.dive@cea.fr.

² The abbreviations used are: MMP, matrix metalloproteinase; Mca, (7-methoxycoumarin-4-yl)acetyl; Dpa, N^3 -(2,4-dinitrophenyl)-L-2,3-diaminopropionyl; DMF, N,N -dimethylformamide; DIC, N,N' -diisopropylcarbodiimide; HOBt, N -hydroxybenzotriazole; Fmoc, N -(9-fluorenyl)methoxycarbonyl; HPLC, high pressure liquid chromatography.

ml·min⁻¹, respectively, with a detection at 230 nm. Each peptide and library was analyzed by electron spray mass spectrometry performed on a Micromass Platform II instrument (Atheris Laboratories, Geneva, Switzerland).

Chemistry

Building Blocks—From (*p*-bromophenyl) phosphinic acid (26) and ethyl α -propargyl acrylate (27), (*p*-bromophenyl) α -propargyl phosphinate (*p*-Br-Ph-[P(O)(OH)]-CH₂-(*R,S*)CH(CH₂-C≡CH)-COOEt; intermediate **A**) was prepared by means of Michael addition (28). Four nitrile oxides were prepared from aldehydes: Ar-CHO → Ar-CH=N-OH → Ar-C≡N⁺-O⁻, where Ar represents phenyl, 4-dimethylaminophenyl, 3-chlorobiphenyl, and 3-phenoxyphenyl, following protocols previously described (24, 29). These aldehydes were commercially available, except for 3-phenoxyphenyl aldehyde, which was prepared according to Ref. 30. The above nitrile oxides and intermediate **A**, subjected to 1,3-dipolar cycloaddition conditions, afforded four isoxazole-containing hydroxyl unprotected phosphinic building blocks *p*-Br-Ph-[P(O)(OH)]CH₂-(*R,S*)CH(**R**)COOEt (intermediates **B1–B4**) (24). Protection of the hydroxyphosphinyl function of the **B** intermediates by the adamantyl group (Ad) and removal of the ethyl ester function by saponification led to the final four *p*-Br-Ph-[P(O)(OAd)]CH₂-(*R,S*)CH(**R**)COOH synthons, where **R** represents (3-phenylisoxazol-5-yl)methyl, (3-[4-dimethylaminophenyl]isoxazol-5-yl)methyl, (3-[3-chlorobiphenyl-4-yl]isoxazol-5-yl)methyl, and (3-[3-phenoxyphenyl]isoxazol-5-yl)methyl (see Scheme 1). Intermediates and final products were purified by column chromatography on silica gel (70–230-mesh; Merck), characterized by ¹H, ¹³C, ³¹P NMR spectroscopy (Varian spectrometer, 200-MHz Mercury model) and by mass spectrometry.

Libraries—Libraries of isoxazole-containing phosphinic peptides of the general formula *p*-Br-Ph-[P(O)(OH)]CH₂-(*R,S*)CH(**R**)-Yaa'-Zaa'-NH₂ (see Scheme 1) were prepared by combinatorial chemistry. Solid-phase syntheses were realized on SynPhase lanterns® (Polyamide, D-series, 7.9 μ mol/lantern, nine stacked disks), bearing an Fmoc-protected acid-labile Rink amide linker, by using a standard Fmoc strategy. Each library of 722 compounds was prepared as a set of 19 sublibraries, spatially addressable, containing 38 compounds in mixture (19 compounds, each present in a mixture of two diastereomers arising from the *R* and *S* configurations of the P₁ residue) (see Scheme 1). Fmoc deprotection of the Rink amide linker was performed with 20% piperidine in DMF (1 ml/lantern, 2 × 10 min). Lanterns were then washed with DMF (2 × 5 min), methanol (1 × 5 min), and dichloromethane (2 × 5 min), dried, and used for coupling steps. The randomized Zaa' (P₃) position was generated from an isokinetic mixture of 19 Fmoc-amino acids, containing the following amino acid ratio: Fmoc-Ala-OH, 1.2 mol %; Fmoc-Arg(2,2,4,6,7-pentamethylidihydrobenzofuran-5-sulfonyl)-OH, 7.2 mol %; Fmoc-Asn(trityl)-OH, 2.2 mol %; Fmoc-Asp(OtBu)-OH, 1.4 mol %; Fmoc-Glu(OtBu)-OH, 2.6 mol %; Fmoc-Gln(trityl)-OH, 4 mol %; Fmoc-Gly-OH, 0.4 mol %; Fmoc-His(trityl)-OH, 12.9 mol %; Fmoc-Ile-OH, 19.2 mol %; Fmoc-Leu-OH, 3 mol %; Fmoc-Lys(Boc)-OH, 5.2 mol %; Fmoc-norleucine-OH, 3.1 mol %; Fmoc-Phe-OH, 3.2 mol %; Fmoc-Pro-OH, 1.8 mol %; Fmoc-Ser(OtBu)-OH, 2.2 mol %; Fmoc-Thr(OtBu)-OH, 7.9 mol %; Fmoc-Trp(Boc)-OH, 12.9 mol %; Fmoc-Tyr(OtBu)-OH, 4.9 mol %; Fmoc-Val-OH, 4.7 mol % (cysteine omitted and methionine replaced by norleucine). Introduction of the Zaa' position was performed using 10 eq of the above isokinetic mixture and HOBt·H₂O (10 eq) and DIC (10 eq) in DMF ([Fmoc-AA-OH] = [HOBt] = [DIC] = 225 mM). After the preactivation step, 19 lanterns were immersed and stirred for 1.5 h at room temperature. Equimolar incorporation of each amino acid was checked by amino acid

analysis. After Fmoc deprotection and washing steps, the 19 lanterns were tagged (combinations of colored spindles and cogs were associated with a specific amino acid) and split into 19 pools to allow parallel incorporation of 19 individual amino acids (premixing protocol: Fmoc-AA-OH (10 eq), HOBt·H₂O (10 eq), and DIC (10 eq) in DMF; [Fmoc-AA-OH] = [HOBt] = [DIC] = 225 mM) for 1 h at room temperature (repeated twice). These 19 lanterns (each containing nine disks) were used to synthesize the sublibraries (19 sublibraries/phosphinic building block). From each lantern, a single disk (0.9 μ mol) was taken to prepare a collection of 19 different tagged disks, each disk containing a defined amino acid in the Yaa' position and a mixture of 19 amino acids in the Zaa' position. After Fmoc removal and washing steps, the 19 disks were immersed in the presence of preactivated phosphinic block (1.5 eq), DIC (3 eq), and HOBt·H₂O (3 eq) in DMF ([HOBt] = [DIC] = 66 mM, [phosphinic block] = 33 mM). After 3 h at room temperature, a second coupling step was performed under the same conditions. After washing steps, each disk was treated for 2.5 h with a solution of 95/2.5/2.5 trifluoroacetic acid/triisopropylsilane/H₂O (300 μ l/disk) and washed with an additional cleavage solution (200 μ l/disk). After concentration, each sublibrary was lyophilized from a CH₃CN/H₂O mixture, leading to a set of 19 sublibraries, with a defined amino acid at the Yaa' position.

Qualitative and Quantitative Aspects—All sublibraries were analyzed by electrospray ionization mass spectrometry (ESI⁺ and ESI⁻). In each library, 19 pseudotripeptides were clearly identified. For isobar compounds, tandem mass spectrometry experiments were performed, confirming the quality of the sublibrary. Concentration of each sublibrary was obtained by amino acid analysis.

Synthesis of Single Compounds—These compounds were synthesized according to the protocol described above. Pure diastereomeric forms of compounds **1** and **2** (see Table 1) were obtained by HPLC purification. The *R* and *S* configurations of the P₁ position in these compounds were assigned as described previously (24). As expected, the diastereomeric form eluting first in HPLC (*S* configuration) turned out to be the most potent toward MMPs.

Synthesis of Fluorogenic Substrate—The substrate was prepared on SynPhase lanterns® by using a standard Fmoc strategy. *N*²-Fmoc-*N*³-2,4-dinitrophenyl-L-2,3-diaminopropionic acid was first incorporated into the solid support using standard coupling conditions (10 eq, 2 × 1.5 h). After sequential incorporation of each amino acid, (7-methoxycoumarin-4-yl)acetyl-proline was incorporated into the peptide sequence (5 eq, 2 × 1.5 h). After cleavage from the lantern, the sample was concentrated and lyophilized from a CH₃CN/H₂O mixture. This substrate was purified by reversed-phase preparative HPLC. Analytical HPLC, UV measurements, and mass spectrometry were used to ascertain the purity and structural correctness of the substrate.

Enzyme Assays and Inhibition Studies

Enzyme inhibition assays were carried out in 50 mM Tris/HCl buffer, pH 6.8, 10 mM CaCl₂, at 25 °C as described before (31). With the exception of MMP-11, all of the assays were performed in black 96-well plates (nonbinding surface plates 3650; Corning Costar). All enzymatic studies were performed in order to remain below 10% of substrate hydrolysis (initial rate conditions). Progress curves were monitored by following the increase in fluorescence at 400 nm ($\lambda_{\text{ex}} = 340$ nm), induced by the cleavage of the Mca-Pro-Leu-Gly-Leu-Dpa-Ala-Arg-NH₂ fluorogenic substrate by MMPs. Fluorescence signals were monitored using a photon-counter spectrophotometer (Fluoroskan Ascent; ThermolabSystems), equipped with a temperature device control and a plate shaker. The conditions of a typical experiment were 200 μ l of buffer, 0.2–0.5 nM

Substrate and Inhibitors of MMP-12

MMP, and a 7.5 μM concentration of the above Mca substrate. In the specific case of MMP-11, assays were performed in quartz cuvettes, with mixing by a magnetic stirrer, using a PerkinElmer Life Sciences 50b spectrophotometer. Mca-Pro-Leu-Ala-Cys(OMeBn)-Trp-Ala-Arg-Dpa-NH₂ was used as substrate, as described before, to monitor the activity of MMP-11 (32). Inhibitors or sublibraries at various concentrations were preincubated with the MMPs 30 min before the addition of substrate. The absolute concentration of inhibitor or sublibrary was determined by amino acid analysis. For each inhibitor or sublibrary, the percentage inhibition was determined in triplicate experiments at three concentrations. Inhibitor concentrations were selected in order to observe a 20–80% range of inhibition. $K_{i(\text{app})}$ values were determined using the method proposed by Horovitz and Levitski (33). This approach explicitly takes into account the

effect of the substrate, enzyme, and inhibitor concentrations and applies to the situation of both standard and tight binding inhibition.

k_{cat}/K_m values were determined from first-order full-time reaction curves ($S \ll K_m$; $S = 0.5 \mu\text{M}$), fitted with the integrated Michaelis-Menten Equation 1, by nonlinear regression,

$$P = S_0 (1 - \exp(-kt)) \quad (\text{Eq. 1})$$

where $k = (k_{\text{cat}}/K_m) \cdot E$, P represents product concentration, and S_0 is substrate concentration at $t = 0$, and E is enzyme concentration. MMP concentrations were determined by titration experiments using a phosphinic peptide inhibitor displaying K_i values lower than 0.1 nM toward MMPs. Cleavage site identification for the hydrolysis of Mca-Pro-Leu-Gly-Leu-Glu-Glu-Ala-Dpa-NH₂ by MMP-12, -9, and -13 was performed by HPLC analysis (Atlantis dC₁₈ 5 μ ; 4.6 \times 150 mm; Waters) coupled to an ionic trap (Esquire HCT, Bruker Daltonics). These experiments demonstrated that these MMPs cleaved only the peptide bond located between the Gly-Leu sequence of this substrate.

Molecular Modeling

The interaction of compound **1** with the catalytic domain of MMP12 was modeled using a protocol based on molecular dynamics with the program CHARMM (version 27) (34). CHARMM force field version 22 was used (35). The starting three-dimensional structure of MMP-12 was that of the catalytic domain of this enzyme in complex with an acetohydroxamic acid inhibitor obtained by x-ray diffraction, Protein Data Bank code 1Y93 (20). The initial position of compound **1** was defined by superimposing the catalytic domain of MMP-11 complexed with the phosphinic inhibitor RXP03, Protein Data Bank code 1HV5 (36) on that of the catalytic domain of MMP-12. The structure of compound **1** was then obtained by modification of the structure of RXP03 using the BUILDER facility of InsightII (Accelrys Inc.). Geometrical and nonbonded parameters for the phosphinic inhibitor were derived from *ab initio* quantum calculations with the program GAUSSIAN98 (37).

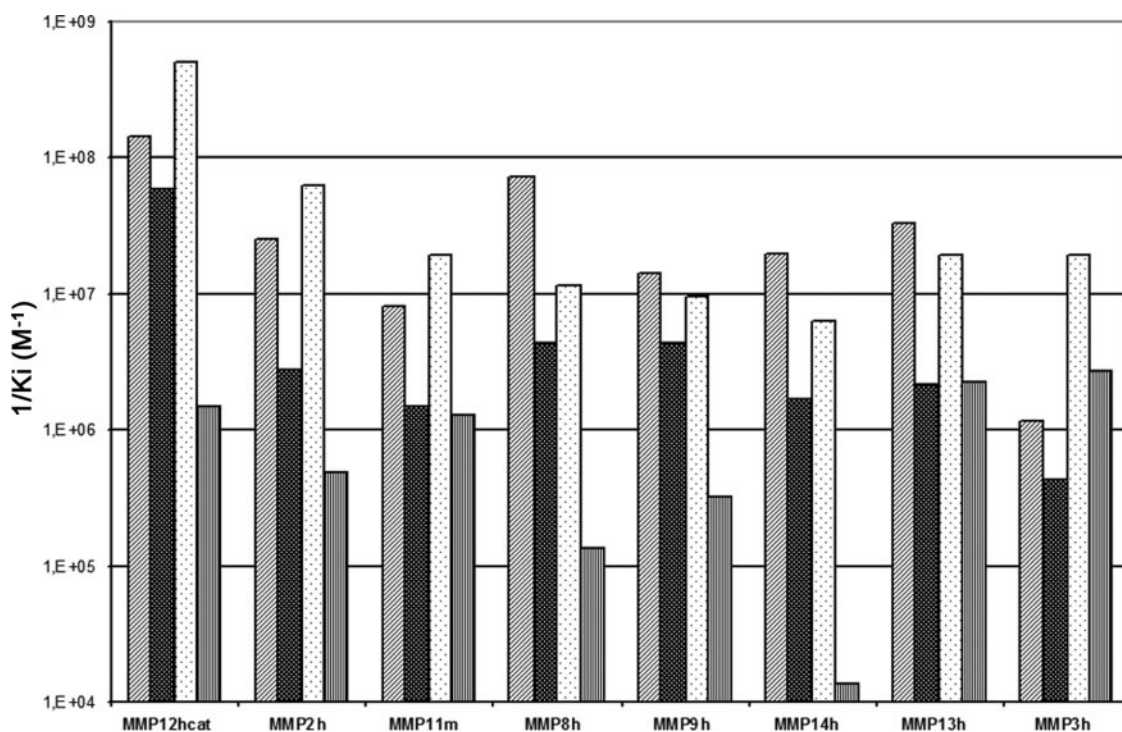
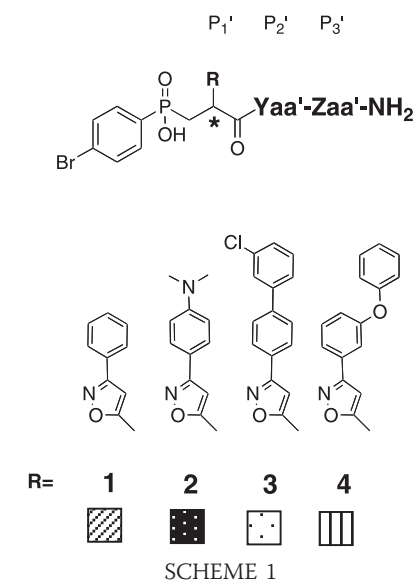


FIGURE 1. Influence of the Xaa' position on the inhibition of MMPs by phosphinic peptide sublibraries of the general formula $p\text{-Br-Ph-(PO}_2\text{-CH}_2\text{)-Xaa'-Phe-Zaa'-NH}_2$. For each MMP, the $1/K_i$ values of the four sublibraries are reported. The fill pattern style defines the Xaa' position, as described in Scheme 1.

These calculations were done at the MP2 level of theory using a 6-31 + $G(d,p)$ basis set. The force constants for the phosphinic inhibitor were approximated to 5 kcal mol⁻¹ rad⁻², 50 kcal mol⁻¹ rad⁻², and 500 kcal mol⁻¹ Å⁻² for the dihedral, bond angle, and bond distance terms, respectively. In order to preserve the structure of the protein during the relaxation of the complex, harmonic restraints were applied to the atomic positions of several sets of atoms. The harmonic constants were set to 30, 10, and 5 kcal mol⁻¹ Å⁻² for the cations (zinc and calcium) and the residues chelating these cations, the nonhydrogen backbone atoms, and the nonhydrogen side chain atoms, respectively. No harmonic restraints were applied to the residues whose atoms were located at a distance greater than 5 Å from the inhibitor's atoms. In addition, a set of distance restraints between the phosphinic inhibitor and the catalytic domain MMP-12 was used in order to preserve the geometry of the hydrogen bond between the main chain of the inhibitor and the protein. During the calculations, the nonbonded interactions were modeled using a Lennard-Jones function and a coulombic electrostatic term with a nonbonded cut-off of 15 Å. The dielectric constant was set to 4. The first step of the relaxation protocol consisted of an initial 2000 cycles of adopted basis Newton-Raphson energy minimization. Then 100,000 steps of molecular dynamics using the Verlet algorithm were calculated. The integration step was set to 0.0005 ps. The temperature was gradually increased by 25 K every 100 steps to reach 450 K. These molecular dynamics calculations were followed by 5000 cycles of energy minimization. The resulting structure was then analyzed with the program PyMOL (Delano).

RESULTS

Four libraries, with the general formula *p*-Br-Ph-(PO₂-CH₂)-Xaa'-Yaa'-Zaa'-NH₂, were synthesized by combinatorial chemistry. They were designed by selecting four different isoxazole side chains in the Xaa' position of the inhibitor to probe the S₁' cavity of MMPs (Scheme 1).

The size of the side chain in the Xaa' position increased from library 1 to 3. In libraries 3 and 4, the side chain in the Xaa' position is of similar size, but, due to para or ortho substitution on the phenyl group attached to the isoxazole ring, the second phenyl group (chlorophenyl or phenoxy) adopts a different orientation, thus probing a different part of the S₁' cavity. Each library was prepared as a set of 19 sublibraries, each containing a single variable amino acid in the Yaa' position, whereas 19 different amino acids in an equimolar mixture were present in the Zaa' position. The determination of the relative potency displayed by each sublibrary enables determination of the preference of MMPs for the Yaa' position (corresponding to the P₂' position of the inhibitor) in each library.

Role of the P₁' Position in Inhibitor Selectivity—Sublibraries tested at 1 μM displayed weak inhibition toward MMP-1 and MMP-7; thus, data for these two MMPs are not shown in Figs. 1 and 2. This low potency is probably related to the presence of a long side chain in the inhibitor P₁' position. In contrast to most MMPs, these two MMPs are known to possess a shallow S₁' cavity (1). Data reported in Figs. 1 and 2 indicate that the presence of a long side chain in the Xaa' position results in the preparation of inhibitor sublibraries exhibiting high potency toward most of the MMPs tested. Sublibrary potency clearly depends on the size of the R side chain and the MMP tested (Fig. 1; for clarity, only the results for the sublibrary Yaa' = Phe are reported in this figure). For MMP-12, inhibitors harboring the R₃ side chain display the highest potency, whereas the lowest potency was observed for inhibitors containing the R₄ group. R₁ and R₂ side chains are well accommodated by MMP-12, with the R₂ substituent providing more selective inhibitors for MMP-12. The preference of MMP-12 for the R₃ group was also observed for MMP-2 and -11, but for these two

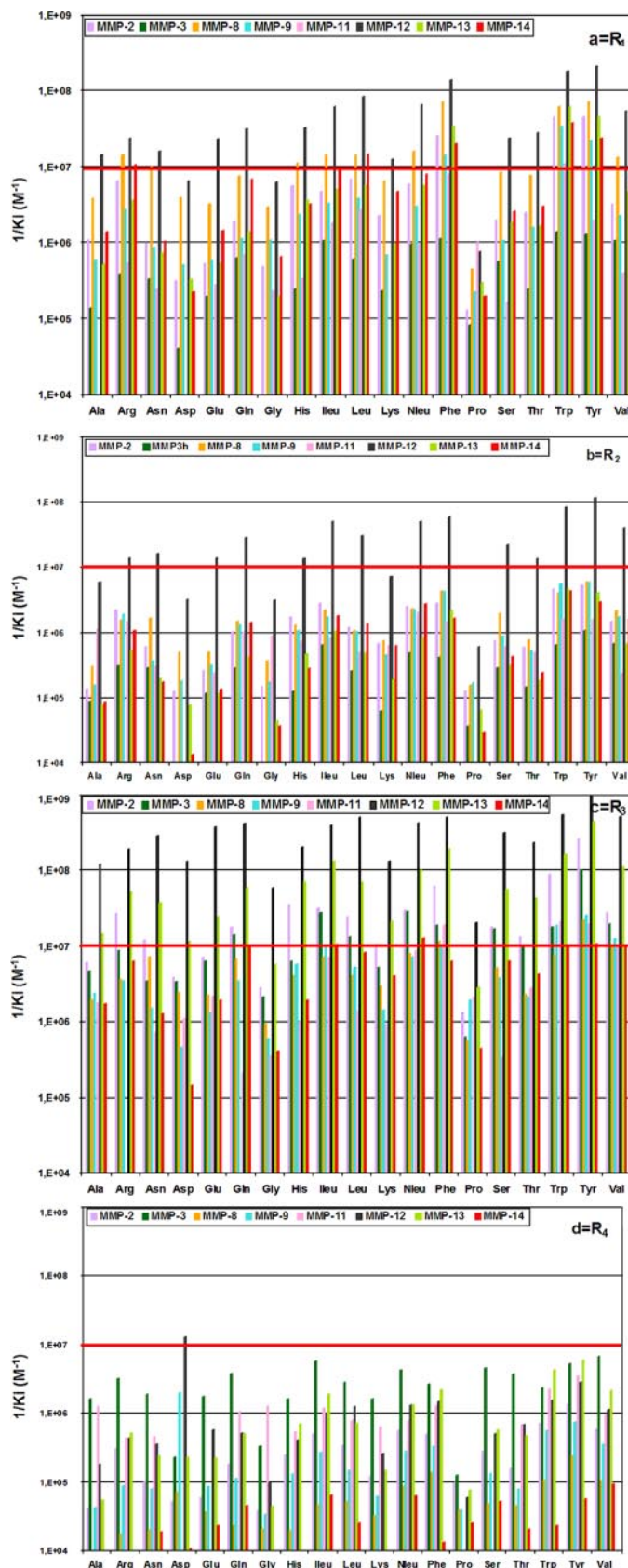


FIGURE 2. Influence of the Yaa' (P₂') position on the inhibition of MMPs by phosphinic peptide sublibraries of the general formula *p*-Br-Ph-(PO₂-CH₂)-Xaa'-Yaa'-Zaa'-NH₂. The first through fourth panels correspond to libraries 1, 2, 3, and 4, respectively, as described in Scheme 1, and define the Xaa' position. The red line indicates a K_i value of 100 nM.

Substrate and Inhibitors of MMP-12

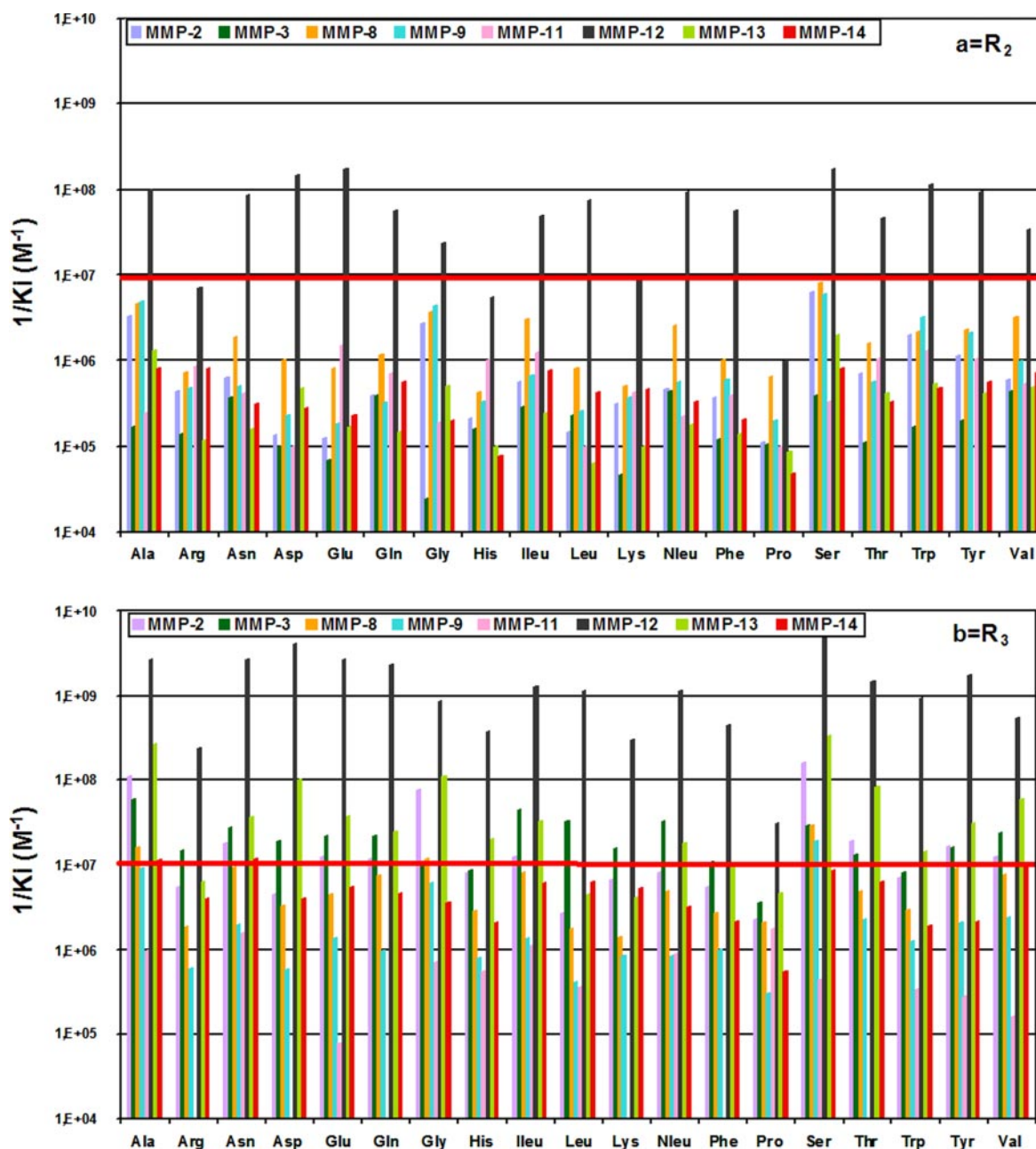


FIGURE 3. Influence of the Zaa' (P_2') position on the inhibition of MMPs by phosphinic peptides of the general formula $p\text{-Br-Ph-(PO}_2\text{-CH}_2\text{)-Xaa'-Glu-Zaa'-NH}_2$. a and b correspond to compounds harboring the Xaa' residue present in libraries 2 and 3, respectively, as defined in Scheme 1. The red line indicates a K_i value of 100 nM.

MMPs, the corresponding inhibitors displayed a reduced potency, as compared with MMP-12 (Fig. 1). MMP-8, -9, -13, and -14 form a group in which the R_1 side chain provides the most potent inhibitors. In this group, inhibitors with R_4 exhibited low potency toward MMP-8 and -9, with MMP-14 being an extreme case. MMP-3 displays a unique inhibition profile, with a preference for R_4 over R_1 and R_2 (Fig. 1). Based on this preference, many sublibraries of inhibitors harboring this R_4 group display good selectivity toward MMP-3 (Fig. 2, fourth panel). But given the weak affinity observed for the corresponding sublibraries, this library was not characterized further. Overall, Fig. 1 illustrates that the presence of the R_2 and R_3 side chains in the inhibitor P_1' position yields compounds that exhibit some selectivity for MMP-12. The same conclusion can be reached by analyzing data reported in Fig. 2.

Role of the P_2' Position in Inhibitor Selectivity—For most MMPs, the presence of an aromatic residue in the P_2' position of the inhibitor enhanced potency, yielding sublibraries that displayed low selectivity (Fig. 2). Proline in the P_2' position yielded sublibraries exhibiting low potency, regardless of the nature of the R group in the P_1' position. As mentioned above, due to the presence of the R_2 side chain, library 2 contains many sublibraries exhibiting selectivity for MMP-12 (Fig. 2, second panel). However, inspection of the library 2 diagrams (Fig. 2, second panel) clearly shows that the nature of the residue in the P_2' position influences the selectivity of inhibitors toward MMP-12. The highest selectivity for MMP-12 was observed when the P_2' position was occupied by a glutamate. Even sublibraries containing a closely related residue such as aspartate and asparagine in the P_2' position appeared less selective. In fact, the presence of a glutamine in the P_2' position gave a

TABLE 1
 K_i values of compounds **1** and **2** towards MMPs (R is defined in Scheme 1)

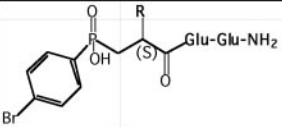
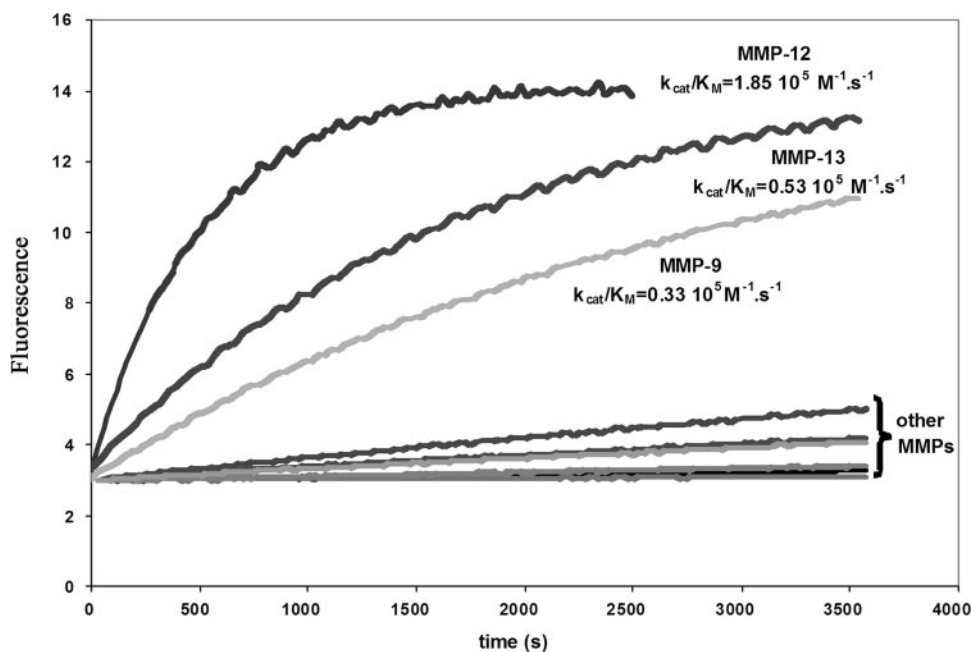
		MMP-1	MMP-2	MMP-3	MMP-7	MMP-8	MMP-9	MMP-11	MMP-12	MMP-13	MMP-14	ACE	NEP	TACE
Compound 1 R=3	K _i (nM)	67000	192	40	626	271	1265	18400	0,19	49	140	>100000	>100000	>100000
	Selectivity/MMP-12	350000	1011	211	3295	1426	6658	96842	1	258	737	>500000	>500000	>500000
Compound 2 R=2	K _i (nM)	>1000000	1673	2724	3472	1338	8286	504	4,4	6524	871	>100000	>100000	>100000
	Selectivity/MMP-12	>22700	380	619	789	304	1883	115	1	1483	198	>22700	>22700	>22700

FIGURE 4. First order full-time reaction curves as observed for the degradation of the Mca-Pro-Leu-Gly-Leu-Glu-Glu-Ala-Dpa-NH₂ (0.5 μM) by MMPs (11 nM), 50 mM Tris, pH 6.8, 10 mM CaCl₂, 25 °C. Nonlinear regression fitting of these curves with the integrated Michaelis-Menten Equation 1 was used to determine the k_{cat}/K_m values for MMP-12, -9, and -13.



sublibrary exhibiting higher potency toward most MMPs, thus decreasing its selectivity toward MMP-12. The sublibrary containing an aspartate was less potent toward MMP-12, so its selectivity was reduced, as compared with the sublibrary with a glutamate.

In library 3, the presence of a glutamate in the P₂' position of the inhibitor also resulted in a sublibrary exhibiting selectivity toward MMP-12, but in this case the sublibrary also exhibited good potency toward MMP-13 (Fig. 2, *third panel*). As shown in Fig. 1, MMP-13 accommodates the R₃ side chain very well in the P₁' position of the inhibitor. Given the good selectivity toward MMP-12 displayed by the mixture of compounds contained in library 2, in particular when the P₂' position is occupied by a glutamate, phosphinic peptides of the general formula *p*-Br-Ph-(PO₂-CH₂)-Xaa'-Glu-Zaa'-NH₂ were prepared, with the Xaa' position occupied by the isoxazole side chain R₂ and the Zaa' position occupied by 19 different amino acids. Similar peptides with the Xaa' position occupied by the R₃ side chain were also synthesized to identify selective MMP-12 inhibitors.

Role of the P₃' Position in Inhibitor Selectivity—When the R₂ chain was present in the Xaa' position, the results reported in Fig. 3a show that the presence of a glutamate in the P₂' position gives several inhibitors displaying high selectivity toward MMP-12, in particular when the Zaa' position is occupied by Asn, Gln, Asp, and Glu, the last inhibitor showing the highest selectivity. Interestingly, selectivity toward MMP-12 is decreased when the Zaa' position is occupied by basic residues. Similarly, with the R₃ side chain in the Xaa' position, the presence of Asn, Asp, Gln, and Glu in the Zaa' position increases the

selectivity of the inhibitors toward MMP-12 (Fig. 3b), leading to a clear differentiation between MMP-12 and MMP-13 (Figs. 2c and 3b).

Compounds 1 and 2 Display High Selectivity toward MMP-12—Due to the presence of an asymmetric center at the P₁' position of the inhibitor, all of the phosphinic peptides reported in this study were prepared as a mixture of two diastereoisomers. Thus, to report potency of the inhibitor in optically pure form, two inhibitors were selected (compounds **1** and **2**, Table 1) and purified by HPLC to resolve these diastereoisomers. Only data for the diastereoisomer exhibiting the shorter retention time in HPLC were reported in Table 1, since this diastereoisomer exhibits the highest selectivity for MMP-12, both for compounds **1** and **2**. A previous study has showed that for this family of isoxazole derivatives, the diastereoisomer eluting first in HPLC possesses the S configuration in the P₁' position (24). Compound **1** with the R₃ group behaves as a highly potent inhibitor of MMP-12 and displays selectivity factors from 2 to 3 orders of magnitude when tested with other MMPs. Compound **2** is less potent toward MMP-12 but displays a similar range of selectivity. Each compound has its own selectivity profile, so, depending on the envisaged application, one compound might be more useful than the other. These results demonstrate that in addition to the size of the isoxazole side chain in the P₁' position, also the presence of a Glu-Glu motif induces selectivity for MMP-12. Moreover, compounds **1** and **2** behave as very weak inhibitors of TACE, NEP, and ACE.

Selective Substrate of MMP-12—To assess further whether a Glu-Glu sequence could be a motif leading to a preferential recognition by MMP-12, this motif was introduced into the sequence of a fluorogenic

Substrate and Inhibitors of MMP-12

peptide. The design of this substrate was based on the structure of a fluorogenic peptide classically used to monitor MMP activity (38) (Scheme 2). MMP-12 was observed to cleave the Glu-Glu substrate with very high efficiency (Fig. 4) and exclusively between the Gly-Leu sequence of this substrate (see "Experimental Procedures"). Thus, when this substrate is cleaved by MMP-12, the Glu-Glu motif interacts with the S_2' and S_3' subsites of MMP-12.



SCHEME 2

In contrast, with the exception of MMP-9 and MMP-13, the Glu-Glu-containing peptide turned out to be a poor substrate of other MMPs, a result illustrating that the Glu-Glu motif may also govern the selectivity of synthetic substrates toward MMP-12 (Fig. 4). Based on the values of the catalytic efficiency parameters (k_{cat}/K_m) reported in Fig. 4, the Glu-Glu substrate is cleaved 3.5 and 5 times more rapidly by MMP-12, as compared with MMP-13 and MMP-9, respectively.

Model of Compound 1 Interacting with MMP-12—A model of compound **1** interacting with MMP-12 was developed to map the residues of MMP-12 that are in close proximity to the Glu-Glu side chains of the inhibitor (Fig. 5). This model reveals that the Glu in the P_2' position is close to Thr²³⁹. Interestingly, with the exception of MMP-7 and MMP-1, MMPs possess bulky hydrophobic residues in place of Thr²³⁹ in MMP-12. As mentioned above, tight interaction of compound **1** with

MMP-1 and MMP-7 is prevented due to the presence of a long side chain in the P_1' position of this inhibitor; thus, the presence of a small polar side chain in these two MMPs, in a position equivalent to Thr²³⁹ in MMP-12, cannot counterbalance the effect of the P_1' residue in this inhibitor.

This model also indicates that the Glu in the P_3' position of compound **1** is in close proximity with Lys¹⁷⁷. With the exception of MMP-2 and MMP-9, most other MMPs do not have a lysine at the MMP-12 equivalent position but a proline. However, in MMP-2 and MMP-9, the lysine residue is followed by an aspartate, whereas in MMP-12 a glycine was observed after the lysine. Inspection of the x-ray structures of MMP-2 and -9 reveals that the aspartate residue in MMP-2 and MMP-9 points toward the P_3' glutamate of the selective inhibitor. Thus, based on this observation, it is tempting to speculate that whereas a favorable interaction between the glutamate of compound **1** and Lys¹⁷⁷ of MMP-12 seems possible, similar interactions would be prevented by the presence of the aspartate residue in MMP-2 and MMP-9, explaining the low potency of compound **1** toward MMP-2 and MMP-9. Inspection of the S_1' loop reveals that the P_1' side chain of compound **1** is in close contact with several residues of this loop. However, two positions occupied by Lys²⁴¹ and Val²⁴³ may deserve particular interest, since a great variability in amino acid composition between the different MMPs is observed for these two positions (Table 2).

DISCUSSION

This study demonstrates that the screening of a limited number of phosphinic peptide sublibraries allows the identification of highly potent and selective inhibitors of MMP-12. In contrast to some hydroxamate derivatives developed for MMP inhibition, the inhibitors reported in this study behave as weak inhibitors of TACE, NEP, and ACE (39). The size of the P_1' residue contributes significantly both to the selectivity and potency of this family of compounds toward MMPs. However, in the particular case of MMP-12, this study demonstrates that the inhibitor selectivity, in addition to the P_1' residue, also depends on the nature of the side chain present in the P_2' and P_3' positions.

Elongation of the R side chain from R_1 to R_2 reduces the inhibitory potency toward MMPs (Fig. 1). This result suggests that some steric hindrance within the MMP S_1' cavity may interfere with the binding of the R_2 group. However, since further elongation of the R group from R_2 to R_3 increases inhibitory potency toward MMPs (Figs. 1 and 2), the reduced potency displayed by the inhibitors in library 2 should involve factors other than steric hindrance. Inspection of the S_1' cavity for most MMPs screened in this study does not reveal the presence of particular residues occluding the cavity, MMP-8 being the sole exception, with an arginine pointing toward the center of the S_1' cavity (Arg²²², MMP-8 numbering). This property may explain the preference of MMP-8 for inhibitors harboring the shortest R group in this series. According to the R side chain preference, MMPs can be assembled in two different groups, one exhibiting a preference for the R_3 side chain and the other for R_1 (Fig. 1). The model of compound **1** in complex with MMP-12 reveals that among the residues of the S_1' loop that are in close proximity to the P_1' residue of compound **1**, two may play a particular role in the preferential recognition of the P_1' residue. These two residues, colored in purple in Fig. 5, are of interest because they are not conserved between

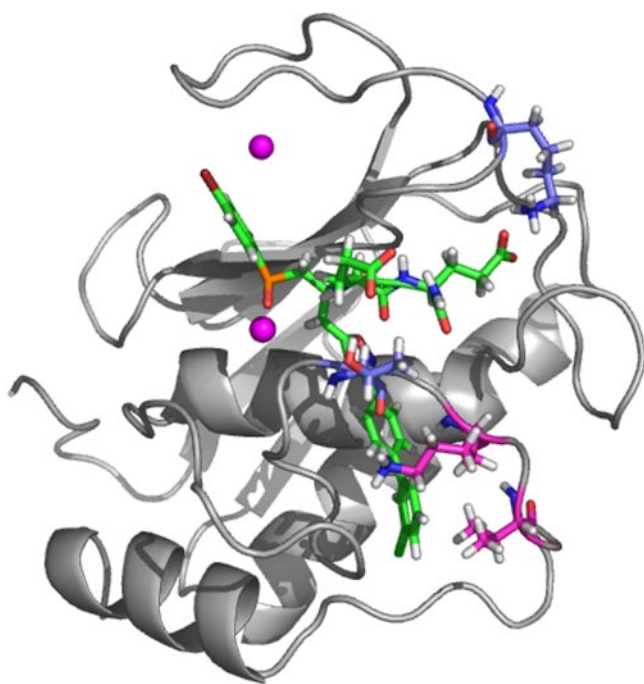


FIGURE 5. **Model of compound 1 in complex with MMP-12.** Residues of MMP-12 in close proximity to the Glu-Glu side chains of compound **1** (in green) are colored in blue. Those in purple correspond to residues of the S_1' loop that differ greatly between the different MMPs. The figure was prepared with PyMOL software.

TABLE 2

Variability in amino acid composition of two positions in the S_1' loop of MMPs (MMP-12 numbering)

Positions	MMP-1	MMP-2	MMP-3	MMP-7	MMP-8	MMP-9	MMP-11	MMP-12	MMP-13	MMP-14
241	Thr	Thr	His	Gly	Ala	Arg	Thr	Lys	Thr	Gln
243	Ser	Thr	Leu	Gly	Arg	Thr	Arg	Val	Thr	Met

MMPs (Table 2). The great diversity of residues in these two positions of the S'_1 loop may influence the binding to MMPs of inhibitors harboring long P'_1 group. However, no simple correlation could be found between these S'_1 residues and the data reported in Figs. 1 and 2. As mentioned in the Introduction, the great flexibility occurring at the level of the S'_1 loop in most MMPs makes it difficult to predict all of the interactions that may take place between P'_1 group and the different residues of the S'_1 loop that point toward the S'_1 cavity. This flexibility, confirmed by recent NMR studies (19, 20), severely limits the use of MMP crystal structures to fully explain the factors contributing to inhibitor potency and selectivity. Mutagenesis experiments will be helpful in assessing the role of these residues in inhibitor recognition. Strikingly, few studies dealing with the role of active site residues of MMPs have been reported (40, 41), and to the best of our knowledge there are none concerning the S'_1 loop residues. Results from such studies may facilitate the selection of the P'_1 side chains that should be introduced into the inhibitor structure to optimize selectivity.

The selective MMP-12 inhibitors reported in this study contain a Glu-Glu motif in their sequence. The side chains of these two Glu are in close proximity to the side chains of Thr²³⁹ and Lys¹⁷⁷, according to our model of compound **1** in interaction with MMP-12 (Fig. 5). The model suggests that the selectivity of compound **1** might be explained either by a direct interaction between the Glu and Thr side chains or alternatively that a hydrophobic residue in position 239, as observed in many MMPs, constitutes an unfavorable environment for the Glu side chain. The fact that Asp and Gln in P'_2 also give rather selective sublibraries argues in favor of the second hypothesis. The same arguments can be used to explain the preference of MMP-12 toward inhibitors possessing a Glu in the P'_3 position. Determination of the MMP-12 structure in complex with compound **1** or **2**, together with mutagenesis experiments, will be necessary to definitively establish the role of Thr²³⁹ and Lys¹⁷⁷ in MMP-12 selectivity. The catalytic efficiency displayed by MMP-12 in cleaving the fluorogenic substrate incorporating the Glu-Glu motif is another observation that illustrates the pivotal role played by this motif in the preferential recognition of a ligand by MMP-12. Further optimization of the sequence of this peptide should lead to substrates exclusively cleaved by MMP-12.

To the best of our knowledge, compounds **1** and **2** are the first examples of highly potent and selective MMP-12 inhibitors (42–44). Several studies have assessed the functional role of MMP-12 in different diseases, using MMP-12-deficient mice. Based on these studies, MMP-12 was proposed to play a key role in the development of emphysema (45–47), atherosclerosis (48–50), and abdominal aortic aneurysm (51, 52). The role of MMP-12 in cancer progression is more elusive (53–55). Given the implication of MMP-12 in different pathologies, it will therefore be of great interest to see whether the development of the corresponding diseases in animal models can be prevented with compounds **1** and **2**.

Screening of a few phosphinic libraries has allowed the identification of highly selective MMP-12 inhibitors. As compared with the hydroxamates, these compounds do not block other proteases such as TACE, ACE, and NEP. These results suggest that selective MMP inhibitors can be selected by screening new phosphinic peptide libraries.

REFERENCES

- Bode, W. (2003) *Biochem. Soc. Symp.* 1–14
- Brinckerhoff, C. E., and Matrisian, L. M. (2002) *Nat. Rev. Mol. Cell Biol.* 3, 207–214
- Mott, J. D., and Werb, Z. (2004) *Curr. Opin. Cell Biol.* 16, 558–564
- Egeblad, M., and Werb, Z. (2002) *Nat. Rev. Cancer* 2, 161–174
- Folgueras, A. R., Pendas, A. M., Sanchez, L. M., and Lopez-Otin, C. (2004) *Int. J. Dev. Biol.* 48, 411–424
- Burrage, P. S., Mix, K. S., and Brinckerhoff, C. E. (2006) *Front. Biosci.* 11, 529–543
- Yong, V. W., Power, C., Forsyth, P., and Edwards, D. R. (2001) *Nat. Rev. Neurosci.* 2, 502–511
- Rosenberg, G. A. (2005) *Lancet* 365, 1291–1293
- Dollery, C. M., and Libby, P. (2006) *Cardiovasc. Res.* 69, 625–635
- Newby, A. C. (2005) *Physiol. Rev.* 85, 1–31
- Whelan, C. J. (2004) *Curr. Opin. Investig. Drugs* 5, 511–516
- Daheshia, M. (2005) *Curr. Med. Res. Opin.* 21, 587–594
- Mannello, F., Tonti, G., and Papa, S. (2005) *Curr. Cancer Drug Targets* 5, 285–298
- Vihinen, P., Ala-aho, R., and Kahari, V. M. (2005) *Curr. Cancer Drug Targets* 5, 203–220
- Tayebjee, M. H., Lip, G. Y., and MacFadyen, R. J. (2005) *Curr. Med. Chem.* 12, 917–925
- Coussens, L. M., Fingleton, B., and Matrisian, L. M. (2002) *Science* 295, 2387–2392
- Brown, S., Meroueh, S. O., Fridman, R., and Mobashery, S. (2004) *Curr. Top. Med. Chem.* 4, 1227–1238
- Cuniasse, P., Devel, L., Makaritis, A., Beau, F., Georgiadis, D., Matziari, M., Yiotakis, A., and Dive, V. (2005) *Biochimie (Paris)* 87, 393–402
- Moy, F. J., Chanda, P. K., Chen, J., Cosmi, S., Edris, W., Levin, J. I., Rush, T. S., Wilhelm, J., and Powers, R. (2002) *J. Am. Chem. Soc.* 124, 12658–12659
- Bertini, I., Calderone, V., Cosenza, M., Fragai, M., Lee, Y. M., Luchinat, C., Mangani, S., Terni, B., and Turano, P. (2005) *Proc. Natl. Acad. Sci. U. S. A.* 102, 5334–5339
- Engel, C. K., Pirard, B., Schimanski, S., Kirsch, R., Habermann, J., Klingler, O., Schlotte, V., Weithmann, K. U., and Wendt, K. U. (2005) *Chem. Biol.* 12, 181–189
- Ikejiri, M., Bernardo, M. M., Meroueh, S. O., Brown, S., Chang, M., Fridman, R., and Mobashery, S. (2005) *J. Org. Chem.* 70, 5709–5712
- Dive, V., Georgiadis, D., Matziari, M., Makaritis, A., Beau, F., Cuniasse, P., and Yiotakis, A. (2004) *Cell Mol. Life Sci.* 61, 2010–2019
- Makaritis, A., Georgiadis, D., Dive, V., and Yiotakis, A. (2003) *Chemistry* 9, 2079–2094
- Kannan, R., Ruff, M., Kochins, J. G., Manly, S. P., Stoll, I., El Fahime, M., Noel, A., Foidart, J. M., Rio, M. C., Dive, V., and Basset, P. (1999) *Protein Expression Purif.* 16, 76–83
- Montchamp, J.-L., and Dumond, Y. R. (2001) *J. Am. Chem. Soc.* 123, 510–511
- Stetter, H., and Kuhlmann, H. (1979) *Synthesis* 1, 29–30
- Yiotakis, A., Vassiliou, S., Jiracek, J., and Dive, V. (1996) *J. Org. Chem.* 61, 6601–6605
- Vogel, A. (1989) in *Vogel's Text Book of Practical Organic Chemistry* (Vogel, A., Furniss, B. S., Hannaford, A. J., Smith, P. W., Tatchell, A. R., eds) pp. 1259 and 1332–1335, John Wiley & Sons, Inc., New York
- Tanaka, A., Terasawa, T., Hagihara, H., Sakuma, Y., Ishibe, N., Sawada, M., Takasugi, H., and Tanaka, H. (1998) *Bioorg. Med. Chem.* 6, 15–30
- Vassiliou, S., Mucha, A., Cuniasse, P., Georgiadis, D., Lucet-Levannier, K., Beau, F., Kannan, R., Murphy, G., Knauper, V., Rio, M. C., Basset, P., Yiotakis, A., and Dive, V. (1999) *J. Med. Chem.* 42, 2610–2620
- Mucha, A., Cuniasse, P., Kannan, R., Beau, F., Yiotakis, A., Basset, P., and Dive, V. (1998) *J. Biol. Chem.* 273, 2763–2768
- Horovitz, A., and Levitzki, A. (1987) *Proc. Natl. Acad. Sci. U. S. A.* 84, 6654–6658
- Brooks, B. R., Bruccoleri, R. E., Olafson, B. D., States, D. J., Swaminathan, S., and Karplus, M. (1983) *J. Comput. Chem.* 4, 187–217
- MacKerell, A. D., Bashford, D., Bellott, M., Dunbrack, R. L., Evanseck, J. D., Field, M. J., Fischer, S., Gao, J., Guo, H., Ha, S., Joseph-McCarthy, D., Kucnhir, L., Kuczera, K., Lau, F. T. K., Mattos, C., Michnick, S., Ngo, T., Nguyen, D. T., Prodhom, B., Reiher, W. E., Roux, B., Schlenkrick, M., Smith, J. C., Stote, R., Straub, J., Watanabe, M., Wiorkiewicz-Kuczera, J., Yin, D., and Karplus, M. (1998) *J. Phys. Chem. B* 102, 3586–3616
- Gall, A. L., Ruff, M., Kannan, R., Cuniasse, P., Yiotakis, A., Dive, V., Rio, M. C., Basset, P., and Moras, D. (2001) *J. Mol. Biol.* 307, 577–586
- Frisch, M. J., Trucks, G. W., Schlegel, H. B., Scuseria, G. E., Robb, M. A., Cheeseman, J. R., Zakrzewski, V. G., Montgomery, J. A., Stratmann, R. E., Burant, J. C., Dapprich, S., Millam, J. M., Daniels, A. D., Kudin, K. N., Strain, M. C., Farkas, O., Tomasi, J., Barone, V., Cossi, M., Cammi, R., Mennucci, B., Pomelli, C., Adamo, C., Clifford, S., Ochterski, J., Petersson, G. A., Ayala, P. Y., Cui, Q., Morokuma, K., Salvador, P., Dannenberg, J. J., Malick, D. K., Rabuck, A. D., Raghavachari, K., Foresman, J. B., Cioslowski, J., Ortiz, J. V., Baboul, A. G., Stefanov, B. B., Liu, G., Liashenko, A., Piskorz, P., Komaromi, R., Gomperts, R., Martin, R. L., Fox, D. J., Keith, T., Al-Laham, M. A., Peng, C. Y., Nanayakkara, A., Challacombe, M., Gill, P. M. W., Johnson, B., Chen, W., Wong, M. W., Andres, J. L., Gonzalez, C., Head-Gordon, M., Replogle, E. S., and Pople, J. A. (2002) *Gaussian 98* (Revision A. 11.3), Gaussian Inc., Pittsburgh, PA
- Knight, C. G., Willenbrock, F., and Murphy, G. (1992) *FEBS Lett.* 296, 263–266
- Saghatelian, A., Jessani, N., Joseph, A., Humphrey, M., and Cravatt, B. F. (2004) *Proc. Natl. Acad. Sci. U. S. A.* 101, 10000–10005
- Welch, A. R., Holman, C. M., Huber, M., Brenner, M. C., Browner, M. F., and Van Wart, H. E. (1996) *Biochemistry* 35, 10103–10109
- Butler, G. S., Tam, E. M., and Overall, C. M. (2004) *J. Biol. Chem.* 279, 15615–15620
- Cook, G. R., Manivannan, E., Underdahl, T., Lukacova, V., Zhang, Y., and Balaz, S.

Substrate and Inhibitors of MMP-12

- (2004) *Bioorg. Med. Chem. Lett.* **14**, 4935–4939
43. Morales, R., Perrier, S., Florent, J. M., Beltra, J., Dufour, S., De Mendez, I., Manceau, P., Tertre, A., Moreau, F., Compere, D., Dublanchet, A. C., and O'Gara, M. (2004) *J. Mol. Biol.* **341**, 1063–1076
44. Dublanchet, A. C., Ducrot, P., Andrianjara, C., O'Gara, M., Morales, R., Compere, D., Denis, A., Blais, S., Cluzeau, P., Courte, K., Hamon, J., Moreau, F., Prunet, M. L., and Tertre, A. (2005) *Bioorg. Med. Chem. Lett.* **15**, 3787–3790
45. Hautamaki, R. D., Kobayashi, D. K., Senior, R. M., and Shapiro, S. D. (1997) *Science* **277**, 2002–2004
46. Morris, D. G., Huang, X., Kaminski, N., Wang, Y., Shapiro, S. D., Dolganov, G., Glick, A., and Sheppard, D. (2003) *Nature* **422**, 169–173
47. Wang, X., Inoue, S., Gu, J., Miyoshi, E., Noda, K., Li, W., Mizuno-Horikawa, Y., Nakano, M., Asahi, M., Takahashi, M., Uozumi, N., Ihara, S., Lee, S. H., Ikeda, Y., Yamaguchi, Y., Aze, Y., Tomiyama, Y., Fujii, J., Suzuki, K., Kondo, A., Shapiro, S. D., Lopez-Otin, C., Kuwaki, T., Okabe, M., Honke, K., and Taniguchi, N. (2005) *Proc. Natl. Acad. Sci. U. S. A.* **102**, 15791–15796
48. Luttun, A., Lutgens, E., Manderveld, A., Maris, K., Collen, D., Carmeliet, P., and Moons, L. (2004) *Circulation* **109**, 1408–1414
49. Morgan, A. R., Rerkasem, K., Gallagher, P. J., Zhang, B., Morris, G. E., Calder, P. C., Grimble, R. F., Eriksson, P., McPheat, W. L., Shearman, C. P., and Ye, S. (2004) *Stroke* **35**, 1310–1315
50. Johnson, J. L., George, S. J., Newby, A. C., and Jackson, C. L. (2005) *Proc. Natl. Acad. Sci. U. S. A.* **102**, 15575–15580
51. Curci, J. A., Liao, S., Huffman, M. D., Shapiro, S. D., and Thompson, R. W. (1998) *J. Clin. Invest.* **102**, 1900–1910
52. Longo, G. M., Buda, S. J., Fiotta, N., Xiong, W., Griener, T., Shapiro, S., and Baxter, B. T. (2005) *Surgery* **137**, 457–462
53. Cornelius, L. A., Nehring, L. C., Harding, E., Bolanowski, M., Welgus, H. G., Kobayashi, D. K., Pierce, R. A., and Shapiro, S. D. (1998) *J. Immunol.* **161**, 6845–6852
54. Hofmann, H. S., Hansen, G., Richter, G., Taege, C., Simm, A., Silber, R. E., and Burdach, S. (2005) *Clin. Cancer Res.* **11**, 1086–1092
55. Kerkela, E., Bohling, T., Herva, R., Uria, J. A., and Saarialho-Kere, U. (2001) *Bone* **29**, 487–493